

Supplementary document for: A correct formulation for the Orientation Dynamic Movement Primitives for robot control in the Cartesian space

Leonidas Koutras

Automation & Robotics Lab
Dept. of Electrical & Computer Engineering
Aristotle University of Thessaloniki, Greece
kleonidas@ece.auth.gr

Zoe Doulgeri

Automation & Robotics Lab
Dept. of Electrical & Computer Engineering
Aristotle University of Thessaloniki, Greece
doulgeri@eng.auth.gr

To demonstrate thoroughly the capabilities of the proposed DMP formulation as opposed to the dominant one, a series of experiments was conducted on a KUKA LWR 4+ robot driven by both the proposed and the dominant formulation. In particular, whenever the case is such that the dominant formulation is not exhibiting any oscillations the performance of the two formulations is expected to be the same. When the dominant formulation exhibits oscillatory performance the proposed formulation is clearly superior. The experimental setup as well as the DMP parameters utilized in all experiments were those given in Section 5 of the paper.

Table 1: TRAJECTORY PARAMETERS

Experiment	Q_0^T	Q_g^T	Figures
A1	$[0.4335 \ -0.3077 \ 0.7387 \ -0.4143]$	$[0.4281 \ -0.0945 \ 0.8352 \ 0.3319]$	1, 2
B1	$[0.6576 \ 0.219 \ 0.7168 \ -0.0764]$	$[0.2486 \ 0.4825 \ 0.5757 \ 0.6115]$	3, 4
C	$[0.557 \ -0.0672 \ 0.8219 \ -0.0985]$	$[-0.1004 \ 0.4323 \ 0.5519 \ 0.706]$	5, 6
D	$[-0.1004 \ 0.4323 \ 0.552 \ 0.706]$	$[0.6577 \ 0.2189 \ 0.7167 \ -0.0765]$	7, 8

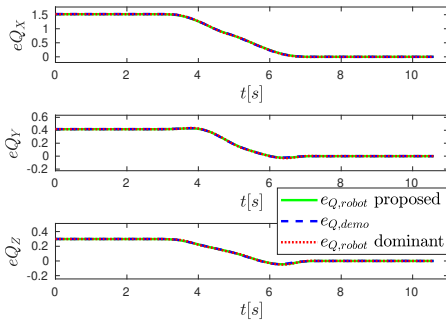


Figure 1: Trajectory A Experiment 1 Result: Evolution of quaternion error with the dominant and the proposed method. The demonstration error trajectory is also depicted.

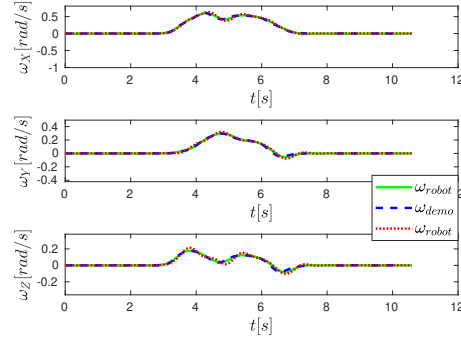


Figure 2: Trajectory A Experiment 1 Result: Evolution of angular velocity with the dominant and the proposed method. The demonstration angular velocity trajectory is also depicted.

Apart from the orientation trajectory presented in the paper, four additional orientation trajectories were recorded and used to train both DMP formulations. Their details are given in Table 1. It is evident from Figures 1 - 8 that the proposed formulation is able to reproduce all four trajectories

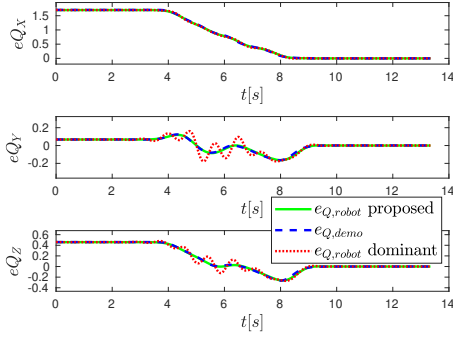


Figure 3: Trajectory B Experiment 1 Result: Evolution of quaternion error with the dominant and the proposed method. The demonstration error trajectory is also depicted.

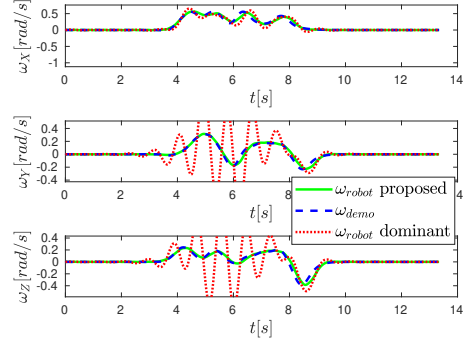


Figure 4: Trajectory B Experiment 1 Result: Evolution of angular velocity with the dominant and the proposed method. The demonstration angular velocity trajectory is also depicted.

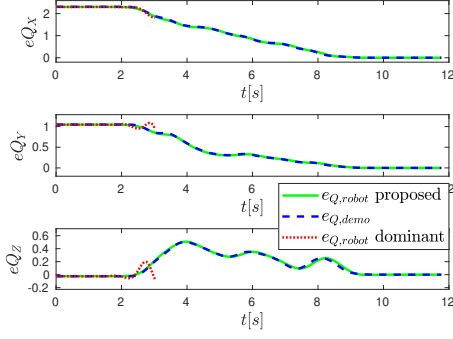


Figure 5: Trajectory C Experiment Result: Evolution of quaternion error with the dominant and the proposed method. The demonstration error trajectory is also depicted.

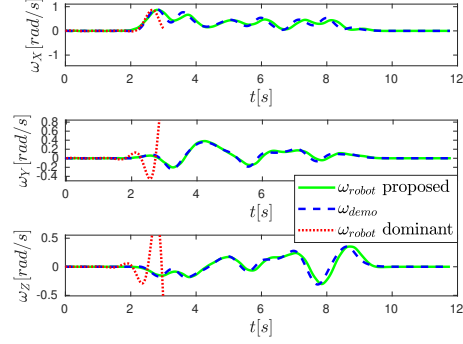


Figure 6: Trajectory C Experiment Result: Evolution of angular velocity with the dominant and the proposed method. The demonstration angular velocity trajectory is also depicted.

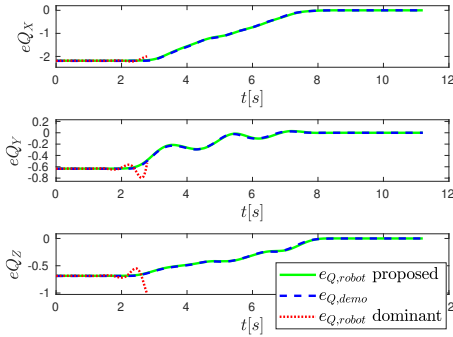


Figure 7: Trajectory D Experiment Result: Evolution of quaternion error with the dominant and the proposed method. The demonstration error trajectory is also depicted.

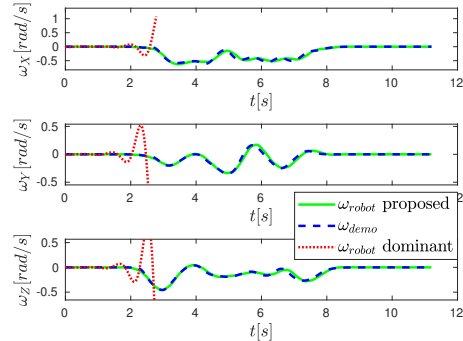


Figure 8: Trajectory D Experiment Result: Evolution of angular velocity with the dominant and the proposed method. The demonstration angular velocity trajectory is also depicted.

accurately while the dominant formulation reproduces accurately only trajectory A; in the rest of the trajectories oscillations appear which may lead to the robot's speed limits violation (trajectory C and D).

In the rest of this supplementary document, experiments were confined to trajectory A and B which were executable by the dominant DMP formulation.

To compare the formulations in a temporal scaling scenario, two experiments were conducted for each of the A and B trajectories. In the first experiment, the temporal scaling parameter was set equal to $\tau = 0.5$, resulting in a trajectory execution in half the duration of the demonstration ($s_\tau = 0.5$). In the second experiment the temporal scaling parameter was set equal to $\tau = 2$, leading to double execution time than the demonstration ($s_\tau = 2$). The results are shown in Figures 9 - 16. Both formulations perform a successful scaled motion. As the oscillations observed with the dominant formulation in trajectory B were also scaled, the faster case ($s_\tau = 0.5$) shown in Figure 13 leads to speed violation and becomes non-executable.

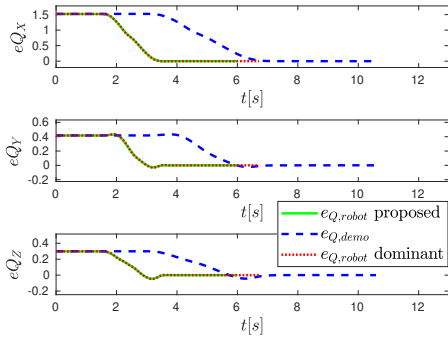


Figure 9: Trajectory A Experiment 2 Result: Evolution of quaternion error with the dominant and the proposed method with $s_\tau = 0.5$. The demonstration error trajectory is also depicted.

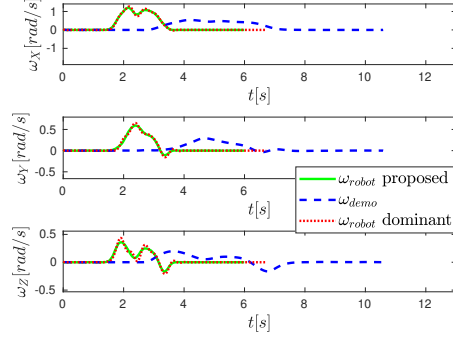


Figure 10: Trajectory A Experiment 2 Result: Evolution of angular velocity with the dominant and the proposed method with $s_\tau = 0.5$. The demonstration angular velocity trajectory is also depicted.

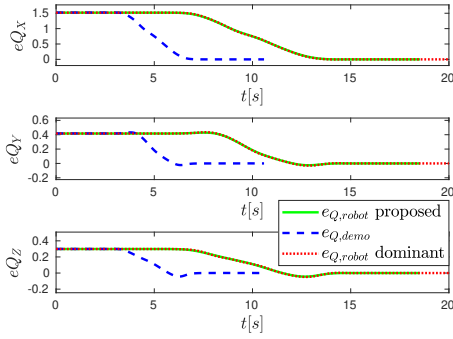


Figure 11: Trajectory A Experiment 3 Result: Evolution of quaternion error with the dominant and the proposed method with $s_\tau = 2$. The demonstration error trajectory is also depicted.

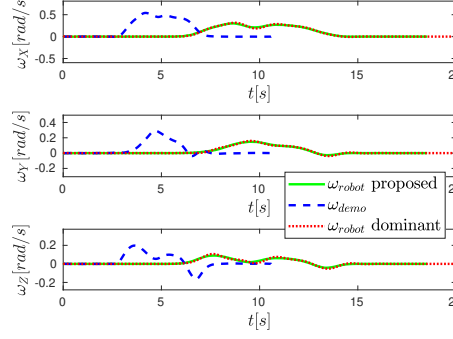


Figure 12: Trajectory A Experiment 3 Result: Evolution of angular velocity with the dominant and the proposed method with $s_\tau = 2$. The demonstration angular velocity trajectory is also depicted.

To test the spatial scaling properties of both formulations new goals for each trajectory were set, yielding a variety of scalings shown in Table 2. Results are shown in Figures 17 - 30. It is clear that the proposed formulation achieves the desired scaling in every case. However, the dominant formulation's behaviour is erratic, as it successfully scales the trajectory towards some goals, as

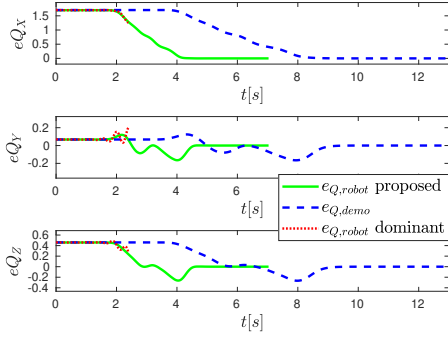


Figure 13: Trajectory B Experiment 2 Result: Evolution of quaternion error with the dominant and the proposed method with $s_\tau = 0.5$. The demonstration error trajectory is also depicted.

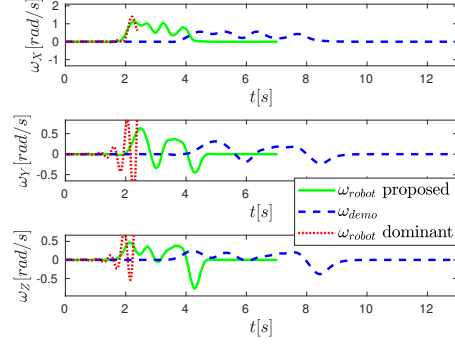


Figure 14: Trajectory B Experiment 2 Result: Evolution of angular velocity with the dominant and the proposed method with $s_\tau = 0.5$. The demonstration angular velocity trajectory is also depicted.

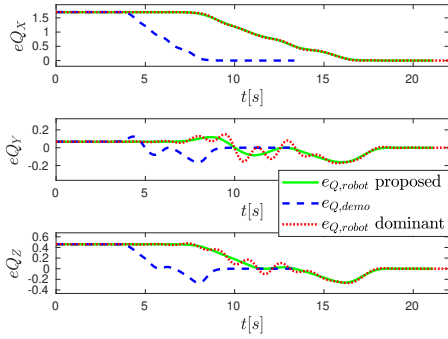


Figure 15: Trajectory B Experiment 3 Result: Evolution of quaternion error with the dominant and the proposed method with $s_\tau = 2$. The demonstration error trajectory is also depicted.

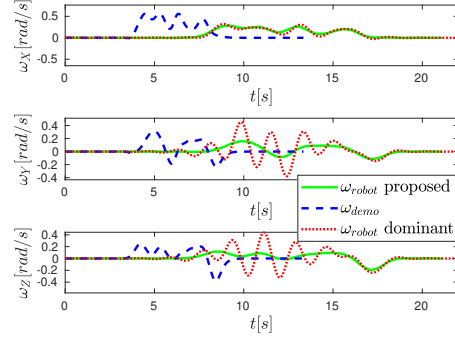


Figure 16: Trajectory B Experiment 3 Result: Evolution of angular velocity with the dominant and the proposed method with $s_\tau = 2$. The demonstration angular velocity trajectory is also depicted.

shown in Figures 19, 20, 23, 24, 27, 28, and it oscillates towards others, as shown in Figures 17, 18, 21, 22, 25, 26, 29, 30 with the case of Figures 25, 26 being prematurely terminated due to the violation of the robot's speed limits. In fact, while trajectory A was executed successfully by the dominant DMP, oscillations appear in 2 out of 3 new goals (Figures 17, 18, 21, 22) while in the execution of trajectory B which exhibited oscillations, the execution was accurate in 2 out of 4 new goals (Figures 23, 24, 27, 28).

For the final experiment we test the DMP formulations under perturbations. During the DMP execution, a human user causes a perturbation as he/she stops the robot and changes its orientation. To recover from the perturbation the temporal scaling adaptation technique was used with $\alpha_{p\tau} = 100$. As a human disturbance input was necessary for the robot's trajectory to be modified, the latter was controlled with rotational stiffness $K_R = 30 \text{ Nm/rad}$. We tested this property only for trajectory A, as there is no point in recovering from perturbations when the generated trajectory is already highly deviant than the demonstrated, as in the case of the dominant formulation in trajectory B. Experimental results are presented in Figures 31 - 34. Figures 31 and 33 show the orientation error evolution with the proposed and dominant formulation respectively, whereas Figures 32 and 34 show the temporal scaling adaptation in each experiment which reaches high values in the presence of disturbance and the DMP evolution is effectively stopped. Due to low rotational stiffness small tracking errors appear between the DMP generated trajectory and the real one.

Table 2: SPATIAL SCALING PARAMETERS

Experiment	Q_g^T	S_g	Figures
A4	$[0.3923 \ -0.0395 \ 0.7892 \ 0.471]$	$1.2I_3$	17, 18
A5	$[0.3642 \ -0.4157 \ 0.8249 \ 0.1182]$	$\text{diag}([0.5 \ 1.5 \ 1.8]^T)$	19, 20
A6	$[0.3727 \ -0.145 \ 0.7906 \ 0.4637]$	$\text{diag}([1.1 \ 1.5 \ 1.7]^T)$	21, 22
B4	$[0.3583 \ 0.4551 \ 0.6466 \ 0.4963]$	$0.8I_3$	23, 24
B5	$[0.7639 \ 0.2463 \ 0.596 \ -0.0255]$	$1.2I_3$	25, 26
B6	$[0.371 \ 0.2642 \ 0.6923 \ 0.5598]$	$\text{diag}([0.7 \ 1.5 \ 1.7]^T)$	27, 28
B7	$[0.2662 \ 0.5320 \ 0.5581 \ 0.5785]$	$\text{diag}([1 \ 0.3 \ 0.7]^T)$	29, 30

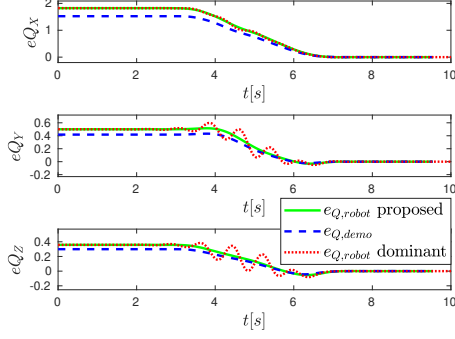


Figure 17: Trajectory A Experiment 4 Result: Evolution of quaternion error with the dominant and the proposed method towards a new goal. The demonstration error trajectory is also depicted.

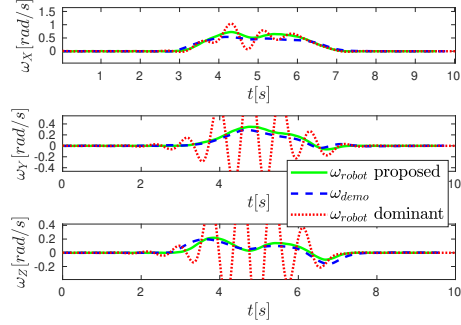


Figure 18: Trajectory A Experiment 4 Result: Evolution of angular velocity with the dominant and the proposed method towards a new goal. The demonstration angular velocity trajectory is also depicted.

The video of all the above experiments can be found in <https://www.youtube.com/watch?v=AFWj58x8veQ>.

Via this extensive experimental study we show that the generated trajectories from the dominant DMP often exhibit an oscillatory behavior that cannot be predicted in advance owing to the tracking error non-linearities which are intrinsic in this formulation. The proposed DMP formulation yields a linear tracking system and as shown in this extensive study it accurately follows the demonstrated and scaled trajectory in each case.

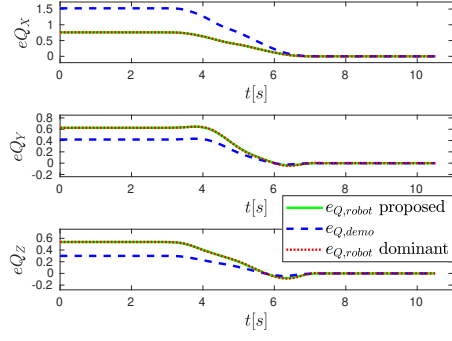


Figure 19: Trajectory A Experiment 5 Result: Evolution of quaternion error with the dominant and the proposed method towards a new goal. The demonstration error trajectory is also depicted.

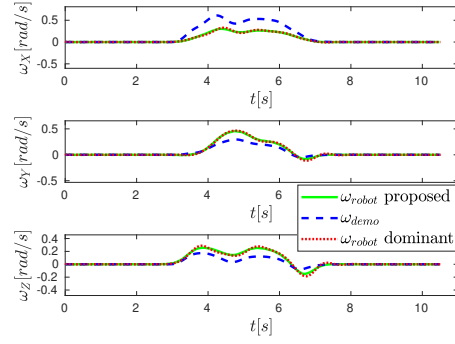


Figure 20: Trajectory A Experiment 5 Result: Evolution of angular velocity with the dominant and the proposed method towards a new goal. The demonstration angular velocity trajectory is also depicted.

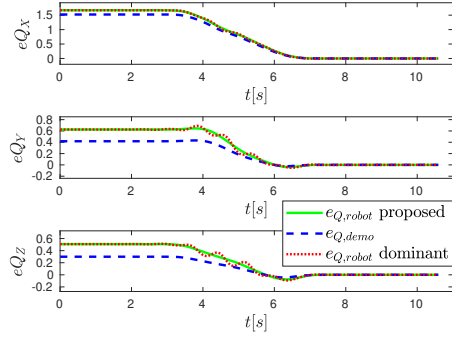


Figure 21: Trajectory A Experiment 6 Result: Evolution of quaternion error with the dominant and the proposed method towards a new goal. The demonstration error trajectory is also depicted.

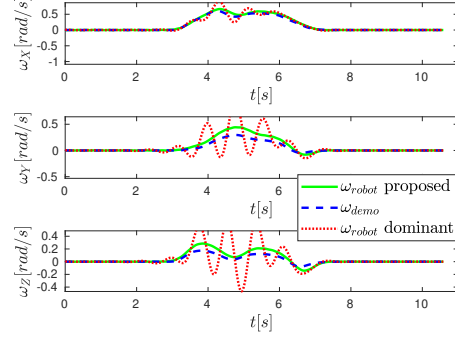


Figure 22: Trajectory A Experiment 6 Result: Evolution of angular velocity with the dominant and the proposed method towards a new goal. The demonstration angular velocity trajectory is also depicted.

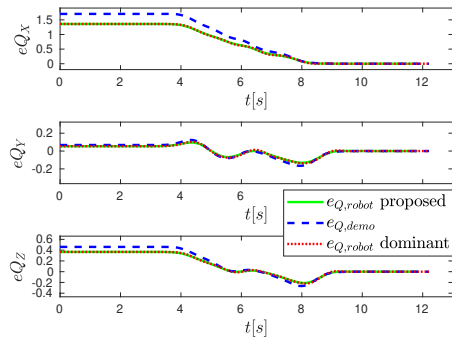


Figure 23: Trajectory B Experiment 4 Result: Evolution of quaternion error with the dominant and the proposed method towards a new goal. The demonstration error trajectory is also depicted.

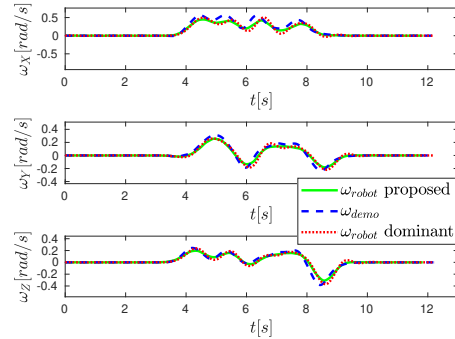


Figure 24: Trajectory B Experiment 4 Result: Evolution of angular velocity with the dominant and the proposed method towards a new goal. The demonstration angular velocity trajectory is also depicted.

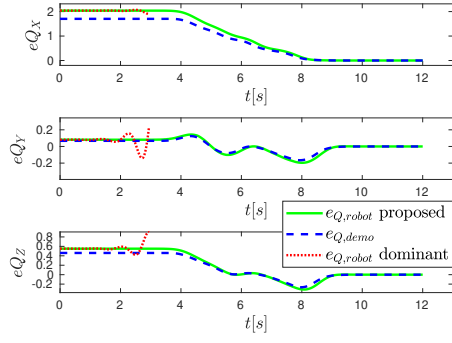


Figure 25: Trajectory B Experiment 5 Result: Evolution of quaternion error with the dominant and the proposed method towards a new goal. The demonstration error trajectory is also depicted.

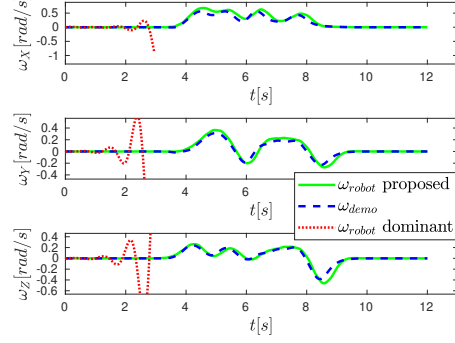


Figure 26: Trajectory B Experiment 5 Result: Evolution of angular velocity with the dominant and the proposed method towards a new goal. The demonstration angular velocity trajectory is also depicted.

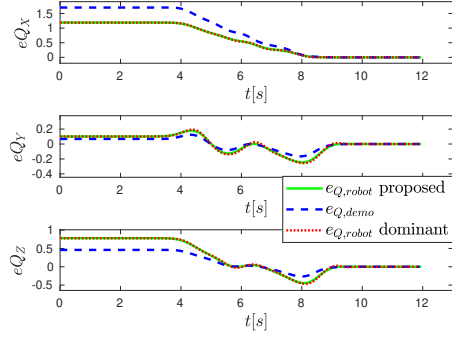


Figure 27: Trajectory B Experiment 6 Result: Evolution of quaternion error with the dominant and the proposed method towards a new goal. The demonstration error trajectory is also depicted.

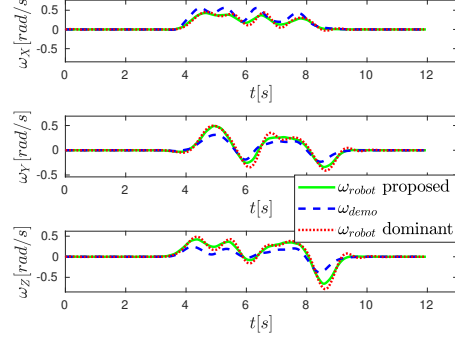


Figure 28: Trajectory B Experiment 6 Result: Evolution of angular velocity with the dominant and the proposed method towards a new goal. The demonstration angular velocity trajectory is also depicted.

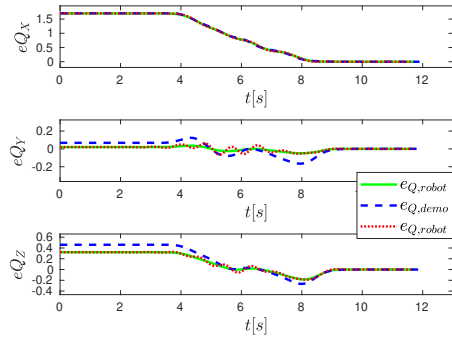


Figure 29: Trajectory B Experiment 7 Result: Evolution of quaternion error with the dominant and the proposed method towards a new goal. The demonstration error trajectory is also depicted.

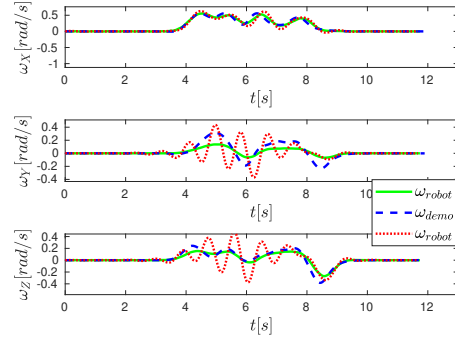


Figure 30: Trajectory B Experiment 7 Result: Evolution of angular velocity with the dominant and the proposed method towards a new goal. The demonstration angular velocity trajectory is also depicted.

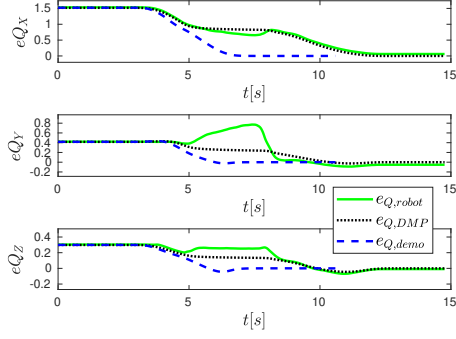


Figure 31: Trajectory A Experiment 7 Result: Evolution of quaternion error with the proposed method under disturbance. The demonstration error trajectory as well as the DMP reference is also depicted.

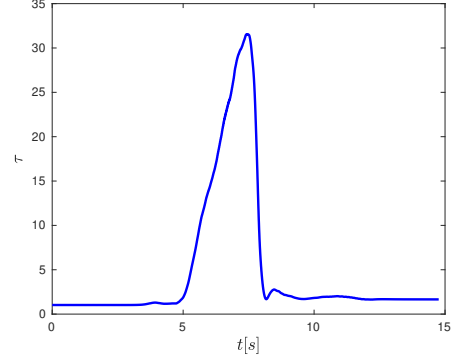


Figure 32: Trajectory A Experiment 7 Result: Adaptation of the temporal scaling parameter during the execution of the proposed method under disturbance.

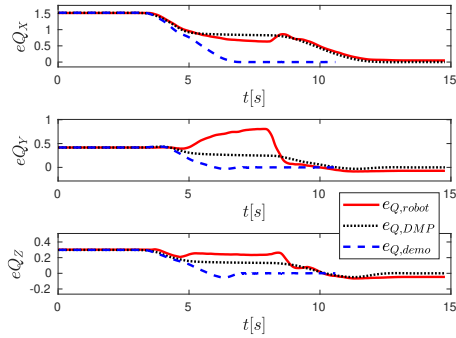


Figure 33: Trajectory A Experiment 7 Result: Evolution of quaternion error with the dominant method under disturbance. The demonstration error trajectory as well as the DMP reference is also depicted.

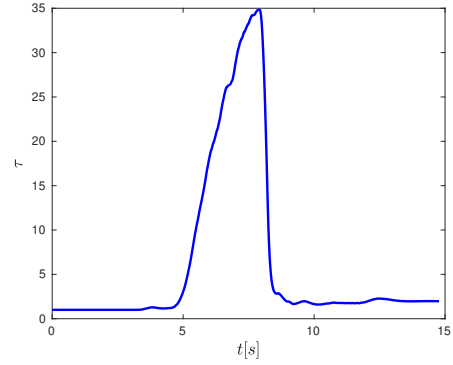


Figure 34: Trajectory A Experiment 7 Result: Adaptation of the temporal scaling parameter during the execution of the dominant method under disturbance.